

See discussions, stats, and author profiles for this publication at: <https://www.researchgate.net/publication/13247817>

Band tails in hydrogenated amorphous silicon and silicon-germanium alloys

Article in *Physical Review Letters* · July 1990

DOI: 10.1103/PhysRevLett.64.2811 · Source: PubMed

CITATIONS

99

READS

203

4 authors, including:



Samer Aljishi

BFG International

67 PUBLICATIONS 869 CITATIONS

[SEE PROFILE](#)



L. Ley

Friedrich-Alexander-University of Erlangen-Nürnberg

499 PUBLICATIONS 28,316 CITATIONS

[SEE PROFILE](#)

Some of the authors of this publication are also working on these related projects:



Study of Thin Film Photovoltaic Semiconductor Materials [View project](#)

Band Tails in Hydrogenated Amorphous Silicon and Silicon-Germanium Alloys

Samer Aljishi,^(a) J. David Cohen,^(b) Shu Jin,^(c) and Lothar Ley^(c)

*Max-Planck-Institut für Festkörperforschung, Heisenbergstrasse 1,
7000 Stuttgart 80, Federal Republic of Germany*

(Received 5 February 1990)

The temperature dependence of the conduction- and valence-band tails has been determined by total-photoelectron-yield spectroscopy for doped and undoped *a*-Si:H and *a*-SiGe:H alloys. We find that all films possess purely exponential conduction- and valence-band-tail densities of states; however, the characteristic energy of the conduction-band tail increases much more rapidly with temperature than that of the valence-band tail. This indicates that the conduction-band tail is considerably more susceptible to thermal disorder than to structural disorder, whereas the reverse holds for the valence-band tail.

PACS numbers: 71.25.Mg, 71.55.Ht

The origin of exponential absorption (Urbach) edges, observed in a large host of crystalline and amorphous semiconductors, is one of the more intriguing problems in basic semiconductor physics. It is generally accepted that its shape largely derives from the exponential falloff into the gap of the conduction- and valence-band densities of states (DOS) which result from static and dynamic site disorder in the material.¹⁻³ In the (hydrogenated) amorphous elemental semiconductors the existence of exponential band tails has been well demonstrated;^{4,5} however, most of what is known about their energy distributions over a range of temperatures has been taken from the analysis of subgap optical-absorption measurements^{1,6} which really represent a convolution of both band tails together.

Recently, Winer and co-workers^{5,7} showed that total-yield-photoelectron spectroscopy can be used to measure separately the energy distribution of valence- and conduction-band-tail states in *n*-type amorphous silicon. In this Letter, we examine the temperature (*T*) dependence of such total-yield spectra in a wide range of doped and undoped *a*-Si:H and *a*-SiGe:H alloys to directly obtain the *energy and temperature* dependence of both the conduction- and valence-band tails in these semiconductors. Thus, for the first time, we may accurately deduce the role of *thermal* and *structural* disorder on the shallow localized gap state distributions for each band-tail region separately and obtain results which contrast markedly with earlier conclusions.

Hydrogenated amorphous silicon (*a*-Si:H) and silicon-germanium alloys (*a*-SiGe:H) were deposited by standard rf (13.56 MHz) glow-discharge decomposition of silane, germane, and hydrogen gas mixtures in an ultrahigh-vacuum reactor. Standard deposition parameters were employed.⁸ Within one minute of the termination of growth, the films were transferred under 2×10^{-10} Torr UHV to the analysis chamber for Kelvin-probe and total-yield measurements. Prior to such measurements all films were annealed at 250°C and then cooled slowly to room temperature.

The Kelvin-probe technique allows the determination of the surface Fermi-level position E_F to within ± 2 meV by measuring the contact potential difference with respect to a vibrating metal reed of known work function.^{5,7} In total-yield spectroscopy, incident uv illumination ($3.5 \text{ eV} < \hbar\omega < 6.4 \text{ eV}$) excites electrons from occupied states in the mobility gap to energies lying just above the vacuum level E_{vac} . As the optical excitation energy $\hbar\omega$ is scanned the total number of photoemitted electrons is counted. The ratio of the number of emitted electrons to the incident photon flux defines the photoelectric yield $Y(\hbar\omega)$. In amorphous solids, $Y(\hbar\omega)$ is simply proportional to a convolution between the occupied DOS, g_{occ} , and a final (unoccupied) DOS above E_{vac} , g_{vac} , weighted by the square of the average dipole matrix element. Because both the transition matrix elements and g_{vac} are well known, we may quite accurately determine the occupied DOS distributions by differentiating the yield data with respect to $\hbar\omega$. To agree with conventional photoemission data, we normalize the occupied DOS to a value of 10^{22} states/eV cm² at a photon energy of 6.2 eV.⁵

In an earlier study we demonstrated that for a fixed optical energy E the occupied DOS a few tenths of an eV above E_F varies with temperature as $\exp[-(E - E_F)/k_B T]$; that is, precisely as expected from thermal occupation statistics.⁹ Hence, it is justified to divide g_{occ} by the Fermi-Dirac occupation function to obtain the *total* DOS, $g(E)$, extending several tenths of an eV above E_F . This offers the unique opportunity to observe *both* the valence- and conduction-band tails in the same sample provided (1) E_F is sufficiently close to the conduction-band edge to provide a measurable occupation of these states, and (2) the photoemission spectra are not appreciably broadened by extraneous sources such as surface-potential variations, inelastic scattering of the photoelectrons, etc. Because of the very large dynamic range of our yield measurements the first condition is easily satisfied in all of our *n*-type doped samples and even some intrinsic films.^{5,9} Regarding the second condition,

we observe that below 190 K our spectra fall off exponentially (above E_F) with a slope of 0.015 eV. This, we believe, establishes a lower limit for resolving the actual energy variations of $g(E)$. Further, because the dominant mechanisms for inelastic scattering (primarily the emission of optical phonons at 57 meV) are nearly independent of temperature, these could not account for the T -dependence effects we observe.

The occupied DOS distributions for several temperatures are shown for a 1000-ppm PH_3 -doped $a\text{-Si:H}$ film in Fig. 1. The spectra display several notable features including a clear shift in the valence-band edge towards E_{vac} with increasing temperature (reflecting the well-known decrease of the optical gap with T), a *temperature-independent* deep-defect band located roughly 5.1 eV below E_{vac} , and an electron density which *decreases continuously* from the valence-band edge (located near 5.7 eV) with decreasing optical energy. In particular, these data indicate that g_{occ} decreases continuously above E_F even for $T > 500$ K. Because the gap-state density is believed to increase exponentially toward the conduction-band mobility edge E_C with a characteristic energy of 35 meV or less, it has been assumed that the occupied DOS would exhibit a peak above E_F at moderate temperatures ($T > 400$ K).¹⁰ Indeed the assumed presence of such a peak has been incorporated into recent attempts to model the dc conductivity and to account for the observed variation in the activation energies of conduction for $T > 450$ K.^{10,11}

The reason that no such peaks appear in our deduced

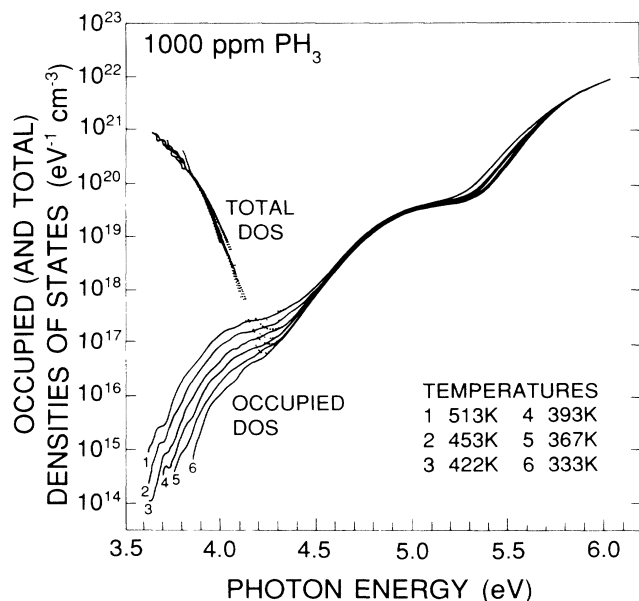


FIG. 1. Occupied (solid curves) and total densities of states (dotted curves) determined from photoelectric-yield spectra for a 1000-ppm PH_3 -doped $a\text{-Si:H}$ sample at six different temperatures. The Fermi-level positions determined by the Kelvin-probe measurements all lie near 4.2 eV.

g_{occ} is made apparent when these distributions are divided by the Fermi occupation function to obtain the total DOS distributions. These are plotted as the dotted lines in Fig. 1. We find, indeed, that for all temperatures, the conduction-band-tail DOS is exponential in energy from slightly above E_F up to approximately 0.3 eV above E_F . However, the total DOS spectra also exhibit a previously unexpected and significant *broadening* with temperature. We define the characteristic energy E_{0C} of the conduction-band tail (CBT) as

$$E_{0C} \equiv [\partial \ln g(\hbar\omega) / \partial (-\hbar\omega)]^{-1}. \quad (1)$$

The condition that a peak appear above E_F in the occupied DOS at temperature T is that $k_B T > E_{0C}$. As a result of the significant broadening of E_{0C} as T is increased, however, this condition is never achieved for this or any other sample studied.

Figure 2(a) displays the full variation of E_{0C} with T for our 1000-ppm P-doped sample as well as for a 50-ppm P-doped sample and an undoped $a\text{-Si:H}$ film. We similarly define and display the T dependence of the valence-band-tail (VBT) characteristic energy E_{0V} in Fig. 2(b) for several undoped and B-doped $a\text{-Si:H}$ films. Figure 2 thus reveals a sharply contrasting behavior between the two band tails; namely, *while E_{0C} increases rapidly with temperature, E_{0V} remains comparatively constant.*

The characteristics of E_{0C} vs T fall into two regimes.

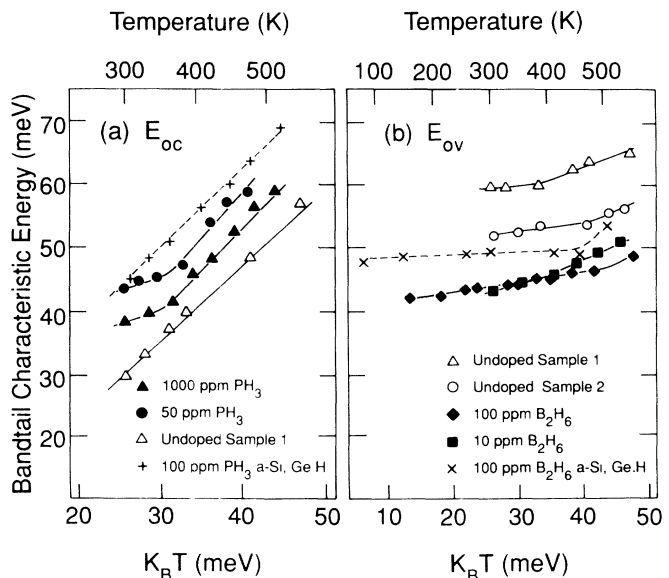


FIG. 2. (a) Characteristic energy E_{0C} vs temperature for the exponential region of the conduction-band tail determined from the total DOS curves such as those displayed in Fig. 1. Results are given for several $a\text{-Si:H}$ samples (solid curves) plus one $a\text{-SiGe:H}$ sample (dashed curve) with $E_{04} = 1.6$ eV. (b) Characteristic energy E_{0V} vs temperature for the valence-band tail for several $a\text{-Si:H}$ samples (solid curves) plus one $a\text{-SiGe:H}$ sample (dashed curve) again with $E_{04} = 1.6$ eV.

Below a temperature T_C^* , E_{0C} is approximately constant (E_{0C}^*) while above T_C^* , E_{0C} increases *linearly* with thermal energy $k_B T$ with a slope that lies in a range between 1 and 2 for different samples. In addition, the extrapolation of the linear portion of $E_{0C}(T)$ intersects the origin ($E_{0C}=0$ at $T=0$). Thus, the functional form of E_{0C} is

$$E_{0C} = \begin{cases} E_{0C}^*, & T < T_C^*, \\ E_{0C}^* T / T_C^*, & T > T_C^*. \end{cases} \quad (2)$$

For the *n*-type films, T_C^* lies in the range 300–360 K. For the undoped sample we could not determine E_{0C}^* and T_C^* due to the much lower thermal occupation of CBT states for $T \leq 300$ K.

By contrast, the valence-band-tail DOS in these samples appears to be little affected by temperature [Fig. 2(b)]. The value of E_{0V} increases by about only 6 meV between 80 and 550 K, which agrees generally with the increase exhibited by the Urbach absorption edge (with characteristic energy E_U) over this same range of temperatures.^{1,12} Indeed, one expects E_U to closely agree with the value of E_0 of the *broader* band tail. Previous studies have demonstrated that one can fit such a temperature variation by the expression

$$E_U = \frac{\hbar \omega_0}{2L} \coth \left[\frac{\hbar \omega_0}{2k_B T} + \frac{1+X}{2} \right], \quad (3)$$

where L is a dimensionless coupling parameter, and $\hbar \omega_0$ is a vibrational energy on the order of the Debye temperature ($\hbar \omega_0 \sim k_B \Theta_D$). Thus, the first term in the square brackets gives the average thermal disorder energy due to the excitation of phonon modes, while X expresses the contribution from *structural* disorder. This equation can be obtained from elementary considerations of the influence of disorder on localized-state energies^{1,2,13} and has also recently been established as part of a more detailed theory by Grein and John.³

Because of the well documented large susceptibility of the valence-band tail to bond-angle deviations, bonded hydrogen configurations, etc.,¹⁴ the second term in Eq. (3) plays the dominant role in determining E_{0V} vs T as deduced by our data. Moreover, a plausible value of $\hbar \omega_0$ of 35 meV is obtained from a fit of E_{0V} vs T by Eq. (3) for the 100-ppm B_2H_6 -doped and -undoped samples [Fig. 2(b)]. On the other hand, applying such a treatment to the E_{0C} vs T data [Fig. 2(a)] seems much less satisfactory. First, we find that the role of structural disorder on the CBT DOS must be nearly zero while the thermal component must be much larger. Given the larger susceptibility of the VBT states to disorder it is somewhat difficult to explain this much stronger coupling to thermal disorder for the conduction-band tail. Second, the rapid linear increase of E_{0C} with T over our temperature range implies that $\hbar \omega_0 \leq 14$ meV for all three films. Finally, such a treatment fails completely to

reproduce the abrupt change in slope at T_C^* exhibited in the E_{0C} temperature dependence.

The experimental results for E_{0C} vs T actually agree much more closely with calculations by Bar-Yam and co-workers^{15,16} which derive the temperature dependence of the exponential band-tail characteristic energies from a thermodynamic ensemble theory of defect dynamics in *a*-Si:H. In that model, the DOS is dictated by thermodynamic equilibrium so that gap states are formed according to the free-energy cost of creating deviations from an ideally bonded network. Such a treatment naturally leads to exponential band tails, a linear dependence of E_{0C} with T , and a characteristic temperature T^* below which the thermal deviations are “frozen in.” This exactly mimics the observed temperature dependence expressed in Eq. (2). The value of T^* is to a degree proportional to the type and extent of disorder.¹⁵ For the *n*-type films measured, we would thus infer that the conduction-band tail exhibits a freeze-in temperature T_C^* which falls between 300 and 360 K. In the undoped films, for reasons discussed above, we can only establish that $T_C^* \lesssim 300$ K. However, our results would be quite consistent with a limiting value of E_{0C}^* near 25 meV, agreeing with values obtained below 250 K for intrinsic samples by time-of-flight measurements.⁴

Adopting such a picture, however, implies once again a fundamental difference between conduction- and valence-band-tail states. That is, the former appear to equilibrate at relatively low temperatures, but this apparently does *not* occur until much higher temperatures for the valence-band tail. Indeed, equilibrium arguments have been used to establish a direct relation between the distribution of VBT states and that of the midgap coordination defects in *a*-Si:H.¹⁷ This is consistent with our results since the deep-defect band, like the distribution of VBT states, varies only slightly over the temperature range studied. Thus we must infer that distinctly different equilibration kinetics govern states in different regions of the mobility gap.

The DOS in *a*-SiGe:H alloys was also investigated. Figure 3 shows the total DOS distribution across the entire gap at several temperatures for a 100-ppm PH_3 -doped *a*-SiGe:H alloy film with a 1.4-eV optical (Tauc) gap ($E_{04}=1.6$ eV). As in *a*-Si:H, both the conduction- and valence-band-tails DOS are purely exponential over several orders of magnitude. The temperature dependences of E_{0C} and E_{0V} (the dashed lines in Fig. 2) closely parallel those observed in *a*-Si:H. In contrast to our *a*-Si:H data, however, the extrapolation of the linear portion of the alloy $E_{0C}(T)$ to zero temperature results in a *finite* intercept of approximately 11 meV (rather than a nearly zero intercept). This may be due to compositional inhomogeneities in *a*-SiGe:H alloys (as discussed by MacKenzie *et al.*¹⁸) which would appear macroscopically as a broadened band tail independent of other structural- or thermal-disorder effects.

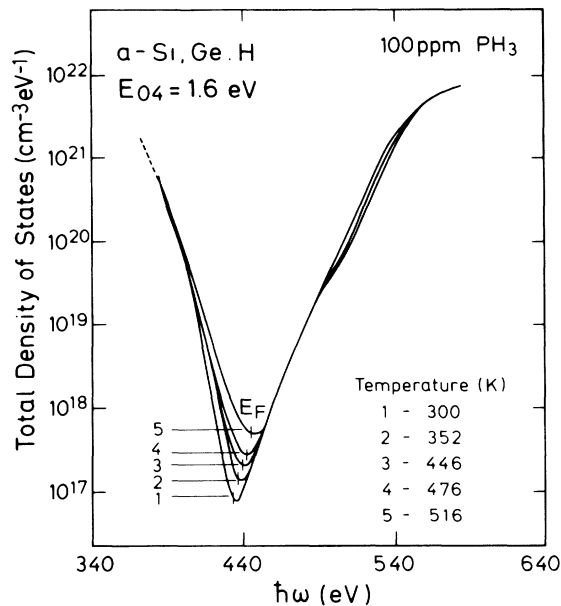


FIG. 3. Total densities of states at five temperatures obtained for a 100-ppm PH_3 -doped $a\text{-SiGe:H}$ sample. The Fermi-level positions are indicated.

Finally, we note that the band-tail DOS data presented here considerably alter the interpretation of the Urbach energies E_U as traditionally measured in these materials. Because it has been assumed that E_{0V} greatly exceeds E_{0C} at all temperatures, the behavior of E_U has been identified exclusively with the valence-band tail. However, we have demonstrated that this is not the case at high temperature where E_{0C} increases dramatically. Some recent measurements of $E_U(T)$ in $a\text{-Si:H}$ have found E_U to be relatively constant below 300 K, but increasing linearly with $k_B T$ (with a slope of almost unity) above 350 K.¹⁹ We strongly suggest that these $E_U(T)$ data actually result from the observed temperature trends of E_{0C} and E_{0V} as indicated from our yield measurements in the low- and high-temperature regimes, respectively.

We are grateful to C. Grein, E. Bustarret, and K. Winer for illuminating discussions. One of us (S.A.) acknowledges the support of a Alexander von Humboldt Foundation fellowship.

^(a)Current address: University of Bahrain, P.O. Box 32038, Bahrain.

^(b)Permanent address: University of Oregon, Eugene, OR 97403.

^(c)Current address: Institut für Technische Physik, Universität Erlangen, 852 Erlangen, Federal Republic of Germany.

¹G. D. Cody, in *Semiconductors and Semimetals*, edited by J. I. Pankove (Academic, New York, 1984), Vol. 21B, p. 11.

²L. Ley, in *Hydrogenated Amorphous Silicon II*, edited by J. D. Joannopoulos and G. Lucovsky (Springer-Verlag, Berlin, 1984), p. 61.

³C. H. Grein and S. John, *Phys. Rev. B* **36**, 7457 (1987); **39**, 1140 (1989).

⁴T. Tiedje, in *Semiconductors and Semimetals* (Ref. 1), Vol. 21C, p. 207.

⁵K. Winer, I. Hiyabayashi, and L. Ley, *Phys. Rev. Lett.* **60**, 2697 (1988); *Phys. Rev. B* **38**, 7860 (1988).

⁶W. B. Jackson, W. M. Kelso, C. C. Tsai, J. W. Allen, and S.-J. Oh, *Phys. Rev. B* **31**, 5187 (1985).

⁷K. Winer and L. Ley, in *Advances in Amorphous Semiconductors: Amorphous Silicon and Related Materials*, edited by H. Fritzsche (World Scientific, Singapore, 1988), Vol. 1, p. 365.

⁸SCCM total flow rate, 250 °C substrate temperature, and 40 mW/cm² power density. (SCCM denotes cubic centimeter per minute at STP.)

⁹S. Aljishi, J. D. Cohen, and L. Ley, *J. Non-Cryst. Solids* (to be published).

¹⁰R. A. Street, J. Kakalios, and M. Hack, *Phys. Rev. B* **38**, 5603 (1988).

¹¹See, for example, H. Overhof, in *Disordered Semiconductors*, edited by M. A. Kastner, G. A. Thomas, and S. R. Ovshinsky (Plenum, New York, 1987), p. 713.

¹²E. Lotter and G. H. Bauer, *J. Non-Cryst. Solids* **114**, 322 (1989).

¹³M. V. Kurik, *Phys. Status Solidi (a)* **8**, 9 (1971).

¹⁴See, for example, D. Allan and J. Joannopoulos, in *Hydrogenated Amorphous Silicon II* (Ref. 2), p. 5.

¹⁵Y. Bar-Yam, D. Adler, and J. Joannopoulos, *Phys. Rev. Lett.* **57**, 467 (1986).

¹⁶Xiaomei Wang, Y. Bar-Yam, D. Adler, and J. Joannopoulos, *Phys. Rev. B* **38**, 1601 (1988).

¹⁷Z. E. Smith and S. Wagner, *Phys. Rev. Lett.* **59**, 688 (1987).

¹⁸K. D. MacKenzie, J. H. Burnett, J. R. Eggert, Y. M. Li, and W. Paul, *J. Non-Cryst. Solids* **97 & 98**, 1019 (1987).

¹⁹G. Weiser and H. Mell, *J. Non-Cryst. Solids* **114**, 298 (1989).